

Approximate Query Processing on Autonomous Cameras

Mengwei Xu
Peking University
mwx@pku.edu.cn

Xiwen Zhang
Purdue ECE
zhan2977@purdue.edu

Yunxin Liu
Microsoft Research
yunxin.liu@microsoft.com

Xuanzhe Liu
Peking University
xzl@pku.edu.cn

Felix Xiaozhu Lin
Purdue ECE
xzl@purdue.edu

ABSTRACT

Surveillance IoT cameras are becoming autonomous: they operate on batteries without connecting to power wires, and run analytics without help from external compute resources. Such autonomous paradigm significantly frees video analytics from privacy concern and deployment constraint. However, they are constrained by limited energy and on-device compute resources.

We present a system AutCam to support counting query, an important query class, on autonomous cameras. The system is built atop three key ideas. First, AutCam identifies and utilizes the rich trade-off between sample quality and sample quantity on a given time window. Second, AutCam introduces a split-phase sampling planner to judiciously allocate energy across multiple time windows, and also balance the capture and process energy. Third, AutCam constructs a unified bounded error by integrating the errors from both sampling and inaccurate neural networks. Tested on over 1,000-hour videos, our prototype of AutCam can provide good estimation of ground-truth object counts with bounded, narrow error under typical solar-harvested energy, and achieve up to 10X energy saving over baselines.

1 INTRODUCTION

IoT cameras are capable of producing colossal videos (16 GBs per camera per day) at low cost (\$20 each), therefore enabling a variety of video analytics [38, 62, 65, 72, 79, 102, 105]. Yet, two major issues block IoT cameras with analytics from being truly pervasive: i) the need for wires, notably for continuous power supply, which raises barriers to camera deployment; ii) privacy concerns, as video footage is uploaded to the cloud and users often have limited, if any, ways for determining and controlling video content [1, 8, 9, 14, 18, 48, 96].

For these reasons, IoT cameras are evolving to be increasingly *autonomous* with two notable trends.

- *Energy independence.* Cameras are capable of operating for long without external power supply. Major smart device vendors, e.g., Netgear, Reolink, Blink, have released popular battery-powered, “wire-free” cameras expected to work for months or years without battery replacement [6, 7, 21]. Commercial cameras solely operating on solar energy also emerge [11, 22].
- *Compute independence.* Cameras execute analytics, such as object detection, on device. They only send concise summaries, e.g.

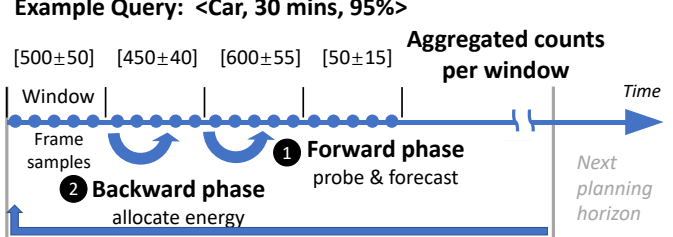


Figure 1: The AutCam workflow, showing a planning horizon.

object counts, to the cloud as requested by users. [5, 10, 11, 15]. Immediately after analytics they delete analyzed videos.

While easing deployment and assuring privacy, autonomous cameras are left with frugal resources, in particular limited energy. For example, a common solar panel (11.5”×6”; harvesting 10Wh per day) can only supply 3% of the energy needed by an embedded platform for object detection at 1 FPS [2]. One may wonder: can autonomous cameras perform any useful video analytics?

To answer this question, we design AutCam, a runtime system for autonomous cameras to continuously count objects in its video feed. Such counting queries provide key information towards understanding video scenes, e.g., human crowd density and vehicle traffic. They enable rich applications, including traffic monitoring [38, 57, 69, 77], public safety [62, 102], wildlife monitoring [55, 79, 82, 94], and smart retailing [4, 65, 72, 105]. As shown in Figure 1, a counting query specifies an object class of interest, e.g., cars, and an aggregation window length, e.g., 30 mins. In response, AutCam generates a stream of aggregated object counts, one for each aggregation window elapsed. The counts are approximate and are accompanied by confidence intervals (CIs), a common notion in approximate query processing (AQP) [35, 36, 42, 46, 49, 100]. The counts are stored on device by default and can be retrieved on demand.

How does AutCam operate? To answer a counting query, AutCam processes sparse samples of image frames, as shown in Figure 1. Over the course of each aggregation window, AutCam periodically wakes up and captures frames. Every N windows (i.e. a planning horizon), AutCam materializes per window aggregated counts: it counts objects on captured frames by running neural nets (called NN object counters) on individual frames; based on per frame object counts, AutCam derives per window *aggregated* counts for all these windows. The notion of planning horizon is common in energy-constrained systems [52]; it gives the systems essential headroom for planning energy use over long timespans.

Our *design goal* for AutCam is to best use limited energy for answering queries with highly confident results, i.e., bounded and low errors. We identify three major design considerations.

(1) *Trade-off between sample quality and quantity* For a window, AutCam may run high-accuracy NN counters on fewer frames (i.e. high quality with low quantity) or low-accuracy NN counters on more frames (i.e. low quality with high quantity). The decision depends on variation in object counts, available energy, and desired confidence in aggregated counts. This challenges AutCam for identifying optimal decisions online. The use of inaccurate counters further challenges AutCam for presenting meaningful error for an aggregated count, as the error comes from two sources: i) that AutCam samples frames rather than processing all available frames; and ii) that the object count on each sampled frames, as returned by inaccurate counters, is inexact. Prior AQP systems focus on the former but never cope with the two sources combined to our knowledge [35, 36, 46].

(2) *Planning sampling across windows* To boost the *overall* confidence in the stream of aggregated counts, AutCam is challenged to pick heterogeneous sample quantities and qualities across windows. For instance, windows with higher object counts and higher count variation deserve denser sampling hence extra energy.

(3) *Frame capturing vs. processing* While AutCam captures frames throughout system operation, as mentioned above it finalizes sampling decisions at the end of each planning horizon, when information of all the horizon's windows becomes available. AutCam is therefore challenged to decide the number of captured frames to match the *future* need in processing. Capturing surplus frames would waste substantial energy, while capturing insufficient frames would miss the opportunity for higher confidence in query answers.

Formulation of AutCam's query planning AutCam plans query execution within the scope of a planning horizon. For a horizon, AutCam decides for each window: the sample quality (NN counter choice) and sample quantity (the numbers of frames to capture and to process). Across all windows of a horizon, these decisions collectively decide the horizon's query confidence (its mean CI width) and its energy consumption. AutCam seeks to either maximize the query confidence with given energy, or to minimize energy to achieve a given confidence target.

To address this problem, AutCam centers on two key techniques as illustrated in Figure 1.

Executing queries: split-phase planning with probes (§4) As shown in Figure 1, instead of deciding a horizon's sample qualities/quantities in one shot, AutCam does so in two phases: at the beginning of each window (❶ the forward phase) and at the end of one entire planning horizon (❷ the backward phase). Furthermore, as each window elapses, AutCam processes a small fraction of frames, called *probes*, as rough estimation of object count and variation in the window.

In the forward phase for a window W , AutCam decides sample *quality* for W ; it does so by learning from historic sample qualities picked when object counts and variations were similar to recent probes. In the backward phase, AutCam decides sample *quantities* for all the windows enclosed in the planning horizon. AutCam does so by allocating energy among the windows iteratively. With

the finalized decisions, AutCam reviews the forecast made in the forward phase and renews its knowledge.

Constructing answers: integrating errors from different sources (§5) AutCam quantifies two errors – the one introduced by frame sampling and the one by inexact object counts on individual frames – as one unified confidence metric. Our key idea is to model the latter error as a random variable. To integrate the errors, AutCam exploits two key characteristics of the variable: independence from the true counts and independence from time. While the integrated error often has an unwieldy form, AutCam uses lightweight approximation to produce confidence intervals. We empirically validate the confidence intervals across a variety of videos.

We build AutCam atop off-the-shelf embedded hardware and test it on over 1000-hour real-world videos. Our results demonstrate its efficacy: powered by a typical solar panel (11.5"×6"), AutCam can continuously produce aggregated object counts for every 30-min window. The counts are only within 11% of the ground truth counts; at 95% confidence level, their CI widths are as narrow as 17% on average. On a typical battery of 150 Watt-hour, AutCam can operate for 15 days, producing aggregated counts with 21% CI width on average. To reach typical CI width as target, AutCam can reduce the overall energy by 4× on average and up to 12.5× compared to the baseline running only the most accurate object detector.

We make the following contributions.

- We identify the emerging scenario of running object counting query on autonomous cameras. We thoroughly investigate sampling decisions and their implications on energy consumption and query confidence.
- We propose a novel mechanism, split-phase planning, for making heterogeneous sampling decisions for individual windows and resolving the tension of frame capturing/processing.
- We propose a novel approach to integrate errors of multiple sources. To our knowledge, we are the first to harness inaccurate neural nets in answering object counting queries with bounded errors.
- We build AutCam, a runtime for executing counting with low errors under limited energy. Atop off-the-shelf embedded hardware, AutCam demonstrates low errors and practical battery life to be useful.

2 BACKGROUND

2.1 Analytics on autonomous cameras

Recent IoT cameras evolve to be more autonomous with two notable trends. i) Many popular cameras require no wires; they operate on harvested energy [11, 22] or pre-charged batteries [6, 7, 21]. ii) They execute video analytics on local device [5, 10, 11, 15].

These trends lead to clear advantages. First, camera deployment is much easier as no infrastructure or continuous connectivity is needed. This particularly suits mass development of inexpensive cameras and in remote areas, e.g. on farms [12]. Second, they provide better privacy assurance, as video data never leave cameras.

The implication on analytics, on the other hand, is to cope with limited resource, primarily energy. For energy-harvesting cameras, a common software design is to forecast energy availability in the

near future [11, 22, 73]. Based on the forecast, the camera software manages harvested energy by imposing energy budgets on camera activities. Hence, the camera seeks to maximize useful work with given energy budget. For battery-powered cameras, it is crucial to reduce battery replacement, which is typically human effort. Therefore, the camera seeks to complete given tasks with minimum energy.

2.2 Object counting on videos

Counting is a key query type extensively studied in AQP [42, 49]. For execution efficiency, query engines often count data items with sampling, and present users with approximate counts accompanied by bounded errors. Query engines commonly present errors as *confidence interval* (CI). With a user-specified confidence level $\alpha\%$, a CI is a numerical range given by the query engine, indicating that the probability of the ground truth count falling in the range is $\alpha\%$. For instance, assuming a user queries car count in the past hour with a 95% confidence level, a CI of $[1000 \pm 100]$ means there is 95% chance that the true car count is between 900 and 1100.

Counting (objects) naturally fits into many use cases of video analytics on IoT cameras.

- In *smart retailing*, people counting helps estimate customers' interest in a product, so that the product placement can be optimized accordingly to increase sales [65].
- For *public safety*, crowd counting helps avoid crowd-related disasters like stampedes during public gathering [62, 102].
- In *transportation*, vehicle counting on urban roads helps traffic management and planning, as many cities have built intelligent transportation systems (ITSs) to solve the severe traffic problems [38, 69, 77].
- For *wildlife study*, animal counting helps ecologists study the distribution and abundance of wildlife animals and better conserve ecosystems [79, 82, 94].

NN-based object counters To provide aggregated object counts over a timespan, a core building block is counting objects on a single image. To do so, a state-of-the-art approach is to execute neural networks as object detectors on frames. In this paper, we refer to these detectors as NN object counters.

NN object counters with high accuracy are energy-hungry. As we have measured, YOLOv3, a popular NN, consumes more than 50J energy in processing one frame on Raspberry Pi 4 [19]. It would consume 1.2 kWh per day to count objects on every frame from an IoT camera (1 FPS). This is two orders of magnitude higher than the energy produced by a 11.5"x6" solar panel commonly seen in embedded systems [20].

Luckily, recent research produces a wide selection of NN object counters with diverse accuracy and compute cost. Table 2 lists the set of popular NN counters we use. We refer to the most accurate one (YOLOv3) as the *golden* NN counter, treating the count it reports on a frame as the *ground truth count* for that frame, as was done in prior work [60]. Compared to the golden counter, a less accurate counter will have false positive/negative in detecting objects, therefore reporting a count different than the ground truth count. That is, the NN counter incurs *error* in its count on that frame.

Params	Semantics	Typical
Query	C The class of objects to count	car, person
	w The length of each aggregation window	30 min
	α The confidence level, i.e. the desired probability of query answers covering ground truth counts	95%
System	1. Energy budget : seek to minimize CI widths with given energy; or 2. CI target : seek to minimize energy consumption to stay below given CI width	1. 30Wh/day 2. 15%
	N The length of a planning horizon	24 hours

Table 1: A summary of AutCam parameters for query and system, respectively.

3 THE AUTCAM OVERVIEW

AutCam is a runtime for executing counting queries on autonomous cameras. The *design goal* of AutCam is to best use limited energy for answering queries with high confidence, i.e., with both bounded and low errors. This problem is never addressed in existing video analytics systems [56, 59, 60, 98, 99, 103] to our knowledge.

3.1 Query

On a camera, AutCam runs a query to continuously count objects in a video stream. The query of AutCam is specified as a tuple of $\langle C, w, \alpha \rangle$ (Table 1).

- *Object class* (C) can be any object class detectable by state-of-the-art NNs. In the current AutCam implementation which uses object detectors trained on the COCO dataset [64], C belongs to 80 common object classes including cars, persons, and bicycles.
- *Aggregation window length* (w) defines the temporal granularity for aggregating object counts.
- *Confidence level* α specifies the desired probability of the query answer covering the ground truth count. Based on the desired probability AutCam generates confidence interval, a bounded error widely adopted in many analytics systems [35, 36, 42, 46, 49, 100].

AutCam answers a query with a stream of aggregated counts, $\{[c_i \pm w_i]\}$. In the sequence, each tuple corresponds to one window; c_i is the mean count for all objects of class C appeared in window i ; w_i is the confidence interval width, which shall cover the true count with $\alpha\%$ probability, e.g., $[1000 \pm 100]$ cars crossing the intersection between 2:00 PM and 2:30 PM. A smaller w indicates higher confidence in the aggregate count and hence a more useful result. Note that aggregation window and CI are well-known concepts widely adopted in popular analytics systems [35, 36, 63].

3.2 Operation

AutCam periodically wakes up, captures and stores video frames. On a small fraction of video frames called probes, AutCam runs NN counters to count objects in order to understand the going-on video contents.

Planning horizon Every N consecutive windows, AutCam materializes the aggregated counts for the N windows. At that moment, AutCam samples frames (in addition to existing probes) from these windows, runs NN counters to count objects on these frames, and

NN Counters	input size	Acc.	Fps
YOLOv3 (Golden, GT) [86]	608x608	33.0	0.10
YOLOv2 [85]	416x416	21.6	0.46
faster rcnn inception-v2 [87]	300x300	28.0	0.25
ssd inception-v2 [68]	300x300	24.0	1.25
ssd mobilenet-v2 [89]	300x300	22.0	1.90
ssdlite mobilenet-v2 [89]	300x300	22.0	2.38

Table 2: The NN counters used in this work. The reported accuracy is the mAP on COCO dataset [64]. The speed is measured on RPI 4 hardware. We notice that the COCO mAP is often not representative enough for their accuracy on real-world videos.

accordingly produces aggregated counts per window. After materialization, AutCam deletes all images for the N windows. The notion of planning horizon (Table 1) gives AutCam essential headroom to optimize energy resource over a timespan much longer than a window; it also assures data privacy, as AutCam never stores images older than a planning horizon.

In each aggregation window, AutCam *uniformly* captures frame. To run NN counters, AutCam *randomly* picks frames from the captured ones. Uniform and random sampling ensure the samples are representative of the whole aggregation window without biased to any time segment [47].

Operating objectives AutCam optimizes its operation within the scope of individual planning horizons, for which:

The **resource** is the camera's energy E , a sum of energy for frame capture and frame processing. Notably, frame capture consumes non-trivial energy as it wakes up camera periodically; it may constitute 30% energy on off-the-shelf embedded platforms as we will show in Section 7. Frame processing energy is dominated by execution of NN object detectors.

The **utility** is the overall confidence in the aggregated counts for all the enclosed windows, characterized as reciprocal to the mean of CI widths of all the counts. Mean CI width is commonly used to characterize the overall confidence in a set of aggregates, as used in prior work [36].

Accordingly, AutCam may operate in two modes as configured by the user at deployment time (Table 1):

- *Energy budget mode*: maximizing utility under energy constraint. This is for energy-harvesting cameras where a high-level energy manager predicts future energy availability (e.g., based on sunlight condition) and allocates energy budget to AutCam every planning horizon. Such energy predictors and managers have been well studied and orthogonal to this work [51, 52, 92, 95]. AutCam respects the budget and seeks to minimize the mean CI width.
- *Target CI mode*: minimizing resource to meet given utility constraint. This is for battery-powered cameras and accuracy-sensitive scenarios. Users set a target mean CI width. AutCam seeks to achieve the target on each planning horizons with the lowest possible energy.

3.3 The query planning problem

Per aggregation window: sample quantity vs. sample quality
The trade-off between sample quantity (number) and sample quality

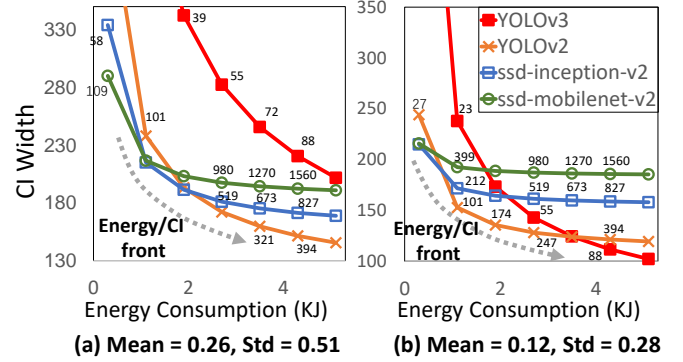


Figure 2: Sampling decision plots for two aggregation windows. On a plot, each point corresponds to a sample quality (the NN counter curve the point is on) and a quantity (numbers annotated along curves). By choosing different sample quality/quantity, AutCam produces diverse CI widths (Y-axis) with different energy consumption (X-axis). All optimal sampling decisions constitute an energy/CI front. Video: Cross.

(accuracy) is a key opportunity of resource allocation of AutCam, as we observed from both statistical perspective (§5) and experiments (following). The trade-off mainly comes from different NN counters (details in Table 2) with diverse accuracy and resource requirement. According to the fundamental statistical theory, with more samples we are able to construct more compact CIs. With given energy, however, the sample quantity is negatively correlated to the sample accuracy, and low sample accuracy hurts the CI.

As a concrete example, we use different NN counters to process two half-hour clips of Cross video (details in Table 3), and report the relationship among energy, CI width, sample quality, and sample quantity. It shows that the most accurate or cheap NN counter does not necessarily lead to the lowest energy consumption or smallest CI width in results. As shown in Figure 2(a), when the energy is low (< 1.0 kJ), ssd-mobilenet-v2 produces the most compact CI. The reason is that at this stage the overall CI width is bounded by the error from sampling, so the cheap NN counter is favored as it provides more sample quantity (> 2× than others). As the energy goes higher, the optimal choice of NN counter also changes (1.0 kJ – 2.0 kJ: ssd-inception-v2; > 2.0 kJ: YOLOv2). Though with more energy the cheap NN counter also receives more samples, but the CI width starts to be bounded by the error from inaccurate NN counters. As a result, the expensive NN counter overtakes the cheap ones.

On a sampling decision plot (shown in Figure 2), all optimal decisions constitute an *energy/CI front*. Any point on the front is a quality/quantity decision that leads to the minimum CI width (Y-axis) with given energy (X-axis), or the minimum energy (X-axis) to stay below a target CI width (Y-axis). The gradient at a point indicates the benefit (reduction in CI width) from additional energy investment. In §5 we will derive an analytic form to depict the front.

Across multiple windows: energy allocation Another dimension of trade-off available to AutCam comes from the disparate

video characteristics across time. Such disparity causes 1) the energy/CI front and the choice of NN counters vary across different aggregation windows, and 2) the return of allocating more energy also varies across aggregation windows. For example in Figure 2, under the same energy budget 2.0 kJ, the optimal NN counters in two video clips are `ssd-inception-v2` and `YOLOv2`. Allocating 1.0 kJ more energy, we can receive 185 CI width reduction in (a) but only 74 in (b). It motivates AutCam to do **global** energy planning across different aggregation windows, instead of allocating statically and uniformly.

As we mathematically study in §5, the video characteristics can be represented by the mean and the standard deviation of the object counts across the aggregation window, often written as (\bar{X}, S) in this paper. In practice, AutCam is not able to get 100% accurate and complete information about the object counts, but approximates them on processed frames.

Summary: the query planning problem Of a planning horizon, aggregation windows are the allocation units that receive resource (energy). AutCam decides for each window: the choice of NN counter and the numbers of frames to capture and process. Across all windows, these decisions collectively decide the horizon's utility (mean CI width) and its energy consumption. AutCam's goal is to either maximize the utility with given energy, or to minimize energy to achieve a given utility target.

4 SAMPLING PLAN

We first discuss ideal, one-phase planning as the baseline (§4.1), illustrating the basic algorithms. Showing the baseline is impractical, we then augment it to be our split-phase planning (§4.2).

4.1 An idealistic design: one-phase planning

Recall that AutCam materializes aggregated counts at the end of each planning horizon. Assume that:

- AutCam knows energy/CI fronts of all aggregation windows.
- AutCam can travel back in time to individual windows for capturing the exact number of frames needed for processing.

Under these impractical assumptions, AutCam makes sampling decisions by solving an energy allocation problem. In doing so, AutCam iteratively allocates energy slices to a window that exhibits the highest CI width reduction given an energy slice. Such an allocation strategy maximizes the planning horizon's utility, which is defined as mean CI width across all windows. Specifically, the allocation works as follows.

- *Initialization*: AutCam dispatches energy to each aggregation window so that each window has a minimum number M of frame samples. This is because in statistics, an estimation from sampling is only regarded meaningful when the sample size is sufficiently large. We pick $M = 30$ by following common practice in statistics [61].
- *Iteration*: In multiple iterations, AutCam allocates small, fixed amounts of energy to individual windows. To pick the next window W for receiving the energy, AutCam examines the energy/CI front of all windows, and selects W to be the one having the front with highest gradient $|\frac{\partial CI}{\partial E}|$. With the energy slice, AutCam increases the sample quantity in W .

- *Terminate*: AutCam reaches the operating constraint: i.e. having depleted the energy budget or met the CI target. At this moment, each window's received energy correspond to the decisions of sampling quantity and quality (the choice of NN counter) for them.

4.2 Split-phase planning

While intuitive, the above one-phase allocation does not work as the assumptions do not hold in reality.

- (1) To get the energy/CI fronts for a window W , AutCam must estimate the object count (\bar{X}, S) for W . This requires AutCam to capture and process a number of frames from W .
- (2) The number of frames available for processing is bound by the number of frames captured. While AutCam cannot decide the number of frames to process until a horizon ends (for optimizing across all the enclosed windows), it has to make capture decision much earlier – before each window.

AutCam makes sample decisions in two separate, yet coupled, phases.

- Forward phase: at the beginning of each window, AutCam decides the number of frames to capture during the window (hence the frame sampling rate), the NN to use over samples from this window;
- Backward phase: at a horizon's end, AutCam decides the number of frames to process for all the windows in the horizon.

Probes AutCam leaves most frame processing at the end of planning horizon when it has an overview of all enclosed aggregation windows. Though, AutCam processes a small number of frames (M) for each aggregation window during forward phase, called probe processing. The reasons for probe are 1) to understand the going-on video characteristics, to help forecast the sample decision for next aggregation window, 2) to bootstrap the energy/CI front of each window, as the initialization stage discussed in the one-phase planning (§4.1).

We now describe how AutCam works in two phases.

4.2.1 The forward phase: forecast. To decide the number of frames to capture for window W , AutCam forecasts the number of frames needed in the backward phase for processing. It does best effort to avoid capturing excessive frames (wasting energy) or insufficient frames (missing opportunity for high confidence).

In general, it is difficult for the forward phase to precisely foresee the sample quantities desired in the backward phase. As shown by the one-phase allocation (§4.1), such a decision for a window W depends on the energy/CI front of W (primary), the constraint for the planning horizon (E or CI) (primary), and the energy/CI fronts of all other windows in the horizon. Our observations are: i) the first two factors have first-order impacts, much higher than the third one; ii) the first factor is primarily determined by video contents. Our rationale is the following: under the same operation constraint (i.e. energy budget or target CI) and for windows with similar object count and variation (\bar{X}, S) , the allocator is likely to allocate a similar amount of energy during backward phase.

AutCam therefore makes the prediction for a window W as illustrated in Figure 3. ① Based on the trend in object counts on recent probes, AutCam (roughly) estimates the object count and variation (\bar{X}, S) in W . With the estimation, AutCam derives energy/CI front for W . ② AutCam checks recent planning history. By referring to

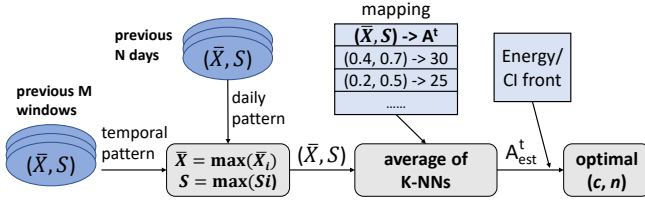


Figure 3: Forward (online) phase of AutCam's planner.

energy allocation received by windows with similar (\bar{X}, S) under similar operation constraint, AutCam predicts the energy that W is likely to receive in the backward planning phase of the current horizon. ③ With the predicted energy allocation, AutCam refers to W 's energy/CI front and determines the frames to process and the choice of object detector, as described in §3.3.

We next describe the steps in detail.

F1. forecast video characteristics (\bar{X}, S) and probes At the beginning of each aggregation window, AutCam forecasts the video characteristics (\bar{X}, S) of upcoming aggregation window. The forecasting is based on two video patterns observed from real-world datasets: (1) *temporal pattern* (immediately precedent windows): the adjacent aggregation windows often have similar video characteristics. (2) *daily pattern* (same time, past days): the video characteristics are often similar to the same time range of past days. To utilize the temporal pattern, AutCam does probe processing, i.e., processes a small number of frames at the end of the previous aggregation window. The NN counter of probe processing is determined ahead of the aggregation window as we will describe in F3. Since the probe processing incurs non-trivial energy cost, typically more than 20% to the overall energy budget, we would like them to be incorporated into the final results.

Given the information from past m days $(\bar{X}_i, S_i, i \in [1, 2, \dots, m])$ and probe results from previous n aggregation window $(\bar{X}'_j, S'_j, j \in [1, 2, \dots, n])$, we need a way to merge those information. Currently AutCam simply uses the average of them.

$$\bar{X}_{est} = \text{mean}(\bar{X}_i, \bar{X}'_j) \quad S_{est} = \text{mean}(S_i, S'_j)$$

F2. forecast global energy allocation To utilize historical knowledge, AutCam manages a mapping about energy allocation decision made at backward phase.

$$\text{mapping} \quad f(\bar{X}, S) \xrightarrow{T} A^t$$

The mapping indicates: under a global operation constraint, how much energy A^t is likely to be received by an aggregation window with (\bar{X}, S) characteristics. The mapping is initialized during bootstrap through an idealistic one-phase planning (§4.1) and continuously calibrated after backward phase (§4.2.2).

To utilize the mapping in online forecast, AutCam takes the k-NN (nearest neighbors) mapping data based on their Euclidean distance with (\bar{X}_{est}, S_{est}) . Denoting the mapping result of those k data points as $(A_1^t, A_2^t, \dots, A_k^t)$, AutCam finally forecasts the energy allocation of the current aggregation window as average of them.

$$A_{est}^t = \text{mean}(A_i^t) \quad i \in [1, 2, \dots, k]$$

F3. forecast frame capture and NN counter choice With the estimated video characteristics (\bar{X}_{est}, S_{est}) and energy allocation (A_{est}^t) likely to be received by current aggregation window, AutCam

picks the NN counter based on the energy/CI front (§3.3). The number of frames to capture can be determined as $n = A_{est}^t / (E(c) + E_{capture})$, where $E(c)$ is the energy consumption of running NN counter c on one frame.

4.2.2 The backward phase. At the end of a planning horizon, AutCam finishes capturing frames from all windows; it has counted objects on a fraction (probes) of these frames; it has decided NN counters for individual windows. $(c_i$ for i -th window). With these results, AutCam executes the backward phase in a simple way.

Similar to the idealistic, one-phase planning, the backward phase iteratively allocates energy slices to the aggregation window with highest confidence return, e.g., CI width reduction $(|\frac{\partial CI}{\partial E}(c_i)|)$. The differences are that (1) since the NN counter is chosen in the forward phase, a window's energy/CI front is reduced to only include the curve for that counter; by allocating more energy, the window's CI width moves on the curve only. (2) AutCam stops considering a window W in allocation after all frames captured in W are processed; (3) after each iteration of energy allocation, AutCam updates the (\bar{X}, S) of the target window by including the new processing results.

Renewing the knowledge Since the overall video contents and system target may change over time, e.g., energy budget changes over different weather conditions, AutCam calibrates the mapping (F2) to adapt to that changing environment. To this end, after each backward phase AutCam reviews the planning decisions, and replays the idealistic planning on the planning horizon. The results may disagree with the decisions have been made on how much energy to allocate to each aggregation window, as we are limited by the realities mentioned at the beginning of §4.2. It then inserts new energy allocation decisions into the mapping f . The old data in the mapping will expire after a certain time period (default: 3 days).

5 INTEGRATING ERRORS FROM MULTIPLE SOURCES

Goal: provide mean object count estimation with CI based on the output from an NN counter on a set of frame samples. The main challenge is how to integrate the error from two different sources: sampling technique and inaccurate NNs. Notice that AutCam doesn't mix NN counters in one aggregation window, as their outputs are difficult to be combined.

- **Input:** the output counts of a given NN counter on a set of image frames $(X_i, i \in [1, 2, \dots, n])$. The frames are randomly sampled within the target aggregation window.
- **Output:** an estimation of the ground-truth mean object counts (μ) within the aggregation window, including the mean and a confidence interval with confidence level α .

According to the statistics theory [47], we have

$$\frac{\bar{X} - \mu_x}{S/\sqrt{n}} \sim T_{n-1} \quad (1)$$

where \bar{X} and S are the mean and standard deviation of X , μ_x is the mean of NN counter output on all the frames in aggregation window, and T_{n-1} is the Student's t-distribution with $n - 1$ degrees of freedom.

However, the NN counter introduces extra error from the ground-truth mean (μ). Thus, We need to model the error to map our observations to the ground truth.

To deal with this challenge, our key idea is to *treat the error of inaccurate NN counter as a random variable that follows a certain distribution, and integrate it with the distribution of sampling result*. Intuitively, the error is proportional to the ground-truth mean value: more objects appear during the aggregation window, more FP and FN tend to be made by the NN counter. Thus, we model the error as the ratio between μ and μ_x ($\mu/\mu_x \sim E_1$). However, we observe that, when the absolute value of μ is too small, the error (ratio) is often very large (outliers). Including those outliers in the overall error distribution will result in very high distribution variance. To eliminate the impacts from those outliers, we set a threshold θ : when μ is smaller than the threshold, we model the error as linear offset between the mean of ground truth and NN counter ($\mu - \mu_x \sim E_2$). In practice, we can use \bar{x} to estimate whether μ is larger than the threshold θ .

We have two key observations about the error distribution of NN counters:

- Error distribution is stable over time. We measure the error of two NN counters (YOLOv2 and ssd mobilenet-v2) on the video stream Jackson. The stream has two separated 1-week video clips with 1-month interval (captured at the first week of May. 2019 and Jun. 2019). The results show that the Bhattacharyya coefficient [39] between the errors of two weeks are 0.93 and 0.86 for two NN counters, respectively. As a result, we can profile the error distribution for once (e.g., when camera is installed) and use it later on.
- Error is independent from X , as confirmed by chi-square test [47] based on the videos we collected. It helps us to simplify the integration of two distributions.

Thus, we have the new distributions (V_1 and V_2) of target μ as following:

$$\mu = \begin{cases} (\bar{x} + S/\sqrt{n} \cdot t) \times e_1 \sim V_1 & \text{if } \bar{x} > \theta \\ (\bar{x} + S/\sqrt{n} \cdot t) + e_2 \sim V_2 & \text{if } \bar{x} \leq \theta \end{cases} \quad (2)$$

$$\text{here : } t \sim T_{n-1}, e_1 \sim E_1, e_2 \sim E_2$$

The distribution of NN counter error (E) can be regarded as a punishment to the resultant CI. Larger error indicates larger $\sigma(E)$, and so more uncertain V distribution, finally results in wider CI. We use μ_{e1}, μ_{e2} to denote the mean of E_1, E_2 . Based on the above, we have the CI of μ as following.

$$\begin{aligned} \text{if } \bar{x} > \theta : CI &= [\bar{x} \times \mu_{e1} - v_{1,\alpha}, \bar{x} \times \mu_{e1} + v_{1,\alpha}] \\ \text{if } \bar{x} \leq \theta : CI &= [\bar{x} + \mu_{e2} - v_{2,\alpha}, \bar{x} + \mu_{e2} + v_{2,\alpha}] \end{aligned}$$

$$\text{where } P(|V_1 - \bar{X} \times \mu_{e1}| \leq v_{1,\alpha}) = \alpha\%$$

$$P(|V_2 - \bar{X} - \mu_{e2}| \leq v_{2,\alpha}) = \alpha\%$$

The CI width, i.e., $v_{1,\alpha}$ and $v_{2,\alpha}$, can be derived through Monte Carlo simulation [88]: randomly picking the same number (N) of samples from t-student distribution and NN counter's error distribution (e_1, e_2) respectively, then combine them as Equation 2. The results, denoted as (y_1, y_2, \dots, y_N) , should follow the target distribution of μ . The CI width, taking $v_{1,\alpha}$ as an example, can be obtained

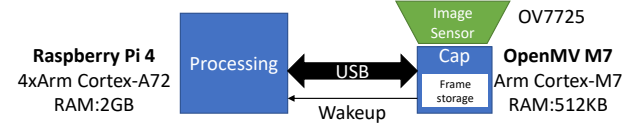


Figure 4: Our hardware prototype for testing AutCam. The platform consists of two SoCs for frame processing & capturing.

as the smallest w that makes the range $[\bar{x} \times \mu_{e1} - w, \bar{x} \times \mu_{e1} + w]$ cover at least $\alpha\% \times N$ data points out of (y_1, y_2, \dots, y_N) .

Approximating μ distribution In practice, one disadvantage of using Monte Carlo simulation to obtain the CI is that it involves intensive computations, especially when it needs to be repeatedly computed in our sampling planning (§ 4). Fortunately, we observe that the distribution of μ is close to normal distributions with similar CDF (cumulative distribution function). Thus, we can approximate the CI width ($v_{1,\alpha}, v_{2,\alpha}$) by treating V_1, V_2 as normal distributions with mean $E(\mu)$ and standard deviation $\sigma(\mu)$.

Based on Equation 2 we can derive the mean and standard deviation of μ as following. Here, μ_{e1}, μ_{e2} are the mean of the NN counter's error distribution E_1, E_2 , and σ_{e1}, σ_{e2} are their standard deviation.

$$\begin{aligned} \bar{x} > \theta : \sigma^2(\mu) &= (\sigma^2(u_x) + \bar{X}^2)(\mu_{e1}^2 + \sigma_{e1}^2) - \bar{X}^2 \mu_{e1}^2 \\ \bar{x} \leq \theta : \sigma^2(\mu) &= \sigma^2(u_x) + \sigma_{e2}^2 \\ \text{where : } \sigma^2(u_x) &= \frac{S^2}{n} \sigma(t_{n-1}) = \frac{S^2(n-1)^2}{n(n-3)^2} \end{aligned} \quad (3)$$

As V_1, V_2 are approximated as normal distributions, we have:

$$v_{1,\alpha}, v_{2,\alpha} = z_{\alpha/2} \sigma(\mu) \quad (4)$$

The approximation also helps us to understand how different factors affect the CI widths $v_{1,\alpha}, v_{2,\alpha}$. It also shows how the CI width reduces when the number of samples increases. It is used to guide AutCam to perform energy allocation across multiple aggregation windows (Section 4).

Convert mean to aggregation (sum) The above shows how to get the mean object count, e.g., “average number of cars crossing the road *each second*”. To convert it to aggregation count, e.g., “total number of cars crossing the road within half hour”, we simply multiply the mean by window size, e.g., $[0.5 \pm 0.1] \rightarrow [900 \pm 180]$ with half-hour window size.

6 IMPLEMENTATION

Hardware platform Commodity IoT cameras are inherently inefficient in capturing a sparse sample of frames: to capture one frame, the whole camera wakes up from deep sleep and falls back to sleep afterwards. This procedure takes several seconds and is energy hungry. On a popular embedded SoC (Cortex-A72), we measured that the energy to capture a frame almost identical to the energy to process the frame (YOLOv2).

While we will test AutCam atop such inefficient hardware, we base most of our experiments on an architecture that offers much higher capture efficiency. As shown in Figure 4, Our architecture

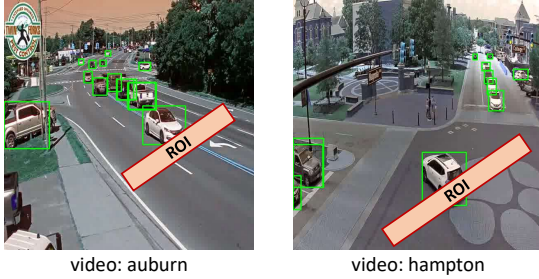


Figure 5: NN-based object counting on region of interest (ROI)

Video	Length	GT count	description
Jackson [27]	2 weeks	1,386/3,060	An intersection in Jackson Hole, WY
Auburn [24]	1 week	495/1,908	Toomers Corner in Auburn, AL
Cross [25]	2 weeks	329/4,412	A three-way cross, location unknown
Taipei [28]	1 week	1,658/4,284	An intersection in Taipei, China
Hampton [26]	1 week	1,267/4,824	An interstate road in Hamptons, NY

Table 3: Videos for evaluation. GT count: mean/max ground truth count of all half-hour windows. Target object: vehicle.

consists of two interconnected SoCs: the capture unit, a microcontroller running RTOS, captures frames periodically with its fast wakeup/suspend; the processing unit, an application processor running Linux, wakes up only to execute NN counters. We believe such a heterogeneous architecture is essential to efficient autonomous cameras.

NN implementations We build the runtime of AutCam based on NNPACK-accelerated darknet [16] (for YOLO NN counters) and TensorFlow [29] (for other NN counters). We use OpenCV [17] for image processing, e.g., resizing.

ROI-based instance counting. As shown in Figure 5, AutCam uses a common way to count object instances by combining object detector output with the specifications of region of interest (ROI) [23, 40]. Since it takes a while, 1 second as an example, for an object to go through the ROI, the object count within a time range is the aggregation of the number of target object overlapping with ROI on all the frames every one second. In practice, though, the counting may have redundancy or miss if the objects move too slow or too fast. It can be further improved by adding more advanced vision algorithm [90]. We leave it as future work as it is out of the scope of our core contributions. Similarly, our system can be easily extended to more prediction targets besides counting instances, e.g., estimating the average vehicle speed [70, 90].

7 EVALUATION

We seek to answer the following questions:

§7.2 Can AutCam provide useful counting estimation with valid, narrow CIs under realistic energy constraints?

§7.3 Whether the key designs of AutCam are significant?

§7.4 How does AutCam react to energy changes?

7.1 Methodology

Videos We evaluate AutCam on 5 video streams captured from different camera feeds, as summarized in Table 3. Each video lasts 1-2 weeks; altogether, they constitute 1176 hours and ~800 GB. We intentionally select the videos to cover diverse real-world scenarios, e.g., urban intersection and interstate highway. Each video is decoded into 1FPS images to work with our ROI-based instance counting (§ 6). We run the golden NN counter on each of those decoded frames to get the ground truth. We use the first two days for bootstrapping AutCam, and the rest of the days for testing.

On these videos, counting objects with low errors is challenging: as most frames contain few objects, the aggregated counts typically show small mean values and high variation. Finding optimal sampling strategies for such sparse data is difficult as shown in previous work [100].

Metrics To quantify AutCam's query answers, we report two main metrics:

- *CI coverage probability.* It is the measured chance that the CIs provided by AutCam cover the ground truth. It is expected to exceed the desired confidence level, as defined in Section 2.
- *Mean CI width,* normalized to the mean count of aggregation window (2rd column in Table 3). For example, for a list of CIs as $[c_i \pm w_i]$, mean CI width is $(\sum w_i)/(\sum c_i)$. A low value indicates high overall confidence in AutCam's query answers.

Furthermore, we report the energy consumed by the whole camera, consisting of both frame capturing and processing.

NN counters and ground truth counts Table 2 lists the NN counters used in experiments. Following prior work [56, 60, 98], we treat as the ground truth the counts returned by the golden NN counter (YOLOv3).

Alternative designs we compared:

• **GoldenNN** runs the golden NN counter with homogeneous sample quantities in all windows. To favor this design, we set an optimal sample quantity, just enough to meet the operation constraint, i.e. energy budget or target CI width, for the whole planning horizon. Note that in practice, a system cannot derive such a quantity as described in Section 4.2. Since GoldenNN introduces no error from NN counter, it can directly derive the CI from the sampling theory (Equation 1).

• **UniNN** runs one single NN counter with homogeneous sample quantities in all windows. To favor this design, we set the NN counter to be the one performing best over all test planning horizons. Similar to GoldenNN, we set sample quantities just enough to satisfy the operation constraint. The design uses our technique (§5) to provide CIs.

• **CapAll** conservatively captures every frame in the video footage (1 FPS). It makes sample decisions with the one-phase strategy described in Section 4.1.

System parameters Unless stated otherwise, we use 30 minutes as the aggregation window [93], and 24 hours as the planning horizon. We use 95% as the default confidence level, a typical number used in prior work [35, 71].

As an important use case, AutCam can operate under limited energy budget harvested from solar power. We used a commercial, compact (11.5 x 6.0 inches), lightweight (0.8 pounds), and economic (< \$30) solar panel to study the typical energy harvested. It shows

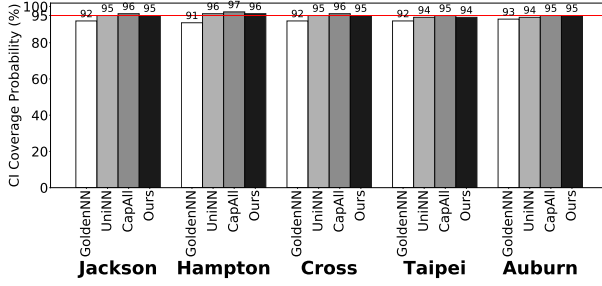


Figure 6: AutCam covers the ground truth at the specified confidence level (95%, the horizontal line).

that $10\text{Wh} \sim 30\text{Wh}$ energy can be harvested by one day in August from the middle of U.S. The number is also consistent with prior work [30].

7.2 End-to-End Performance

Can CIs well cover the ground truth? Figure 6 shows the CI coverage probability. The results are summarized over different experiment setups, i.e., energy budgets and CI width target, as in §7.3. The results show that AutCam (as well as CapAll and UniNN that use our error integration technique) can meet the specified confidence level at 95%. The results validate our technique of error integration (§5).

The CI coverage of GoldenNN is slightly lower than expected. The reason is that, when running under tight energy budget, GoldenNN only processes a very small number of frames (< 30) using the golden NN counter. Such number is not even enough to ensure the results to be statistically meaningful.

Energy budget mode: can AutCam provide useful counts with limited energy? We test AutCam under the typical solar energy budgets. For counting error, the aggregated counts generated by AutCam are with 14.8%, 12.4%, and 11.1% of the ground truth with the energy budgets of 10 Wh/day, 20 Wh/day, and 30 Wh/day, respectively. For counting CI, as shown Figure 7, AutCam presents mean CI widths of 21.9%, 19.1%, and 17.1%, respectively. Such results are comparable to some state-of-the-art video counting approaches and analytics systems [34, 66, 80, 104].

Target CI mode: can AutCam operate reasonably long on batteries? We set the target mean CI widths to be 15%, 20%, and 25%, typical numbers reported in prior work [35, 53, 80]. As shown in Figure 8, the median energy consumptions are 32.9Wh, 17.2Wh, and 9.3Wh per day to achieve the corresponding MCIW. With a commodity rechargeable battery of 150Wh [13] (costs \$46), AutCam is able to continuously count objects for up to a few weeks.

7.3 Validation of Key Designs

7.3.1 Trade-off between sample quality/quantity. (§5) AutCam significantly outperforms GoldenNN, which only uses the highest sample quality (i.e. the golden NN counter). In the energy budget mode shown in Figure 7, AutCam’s mean CI widths are smaller by 58% (with an energy budget of 30Wh/day) and by 69% (with a budget of 10Wh/day) on average. In the target CI mode shown in Figure 8,

AutCam’s energy consumption is lower by 64% (with 15% mean CI width) and 87% (with 25% mean CI width) on average.

Diving deeper, we find that while the golden NN counter ensures high sample quality (i.e. exact counts per frame), AutCam can only afford sampling 30 frames per aggregation window. By contrast, AutCam is able to pick less accurate counters with while sampling $5\text{x} - 9\text{x}$ more frames. The large sample quantities outweigh modestly lower sample qualities and result in overall gain.

7.3.2 Heterogeneous sample decisions across windows. (§4) AutCam significantly outperforms UniNN, which makes static sample decision across all aggregation windows (i.e., optimal but fixed NN counter). In the energy mode shown in Figure 7, AutCam’s CI width is smaller by 19% (with a budget of 30Wh/day) and 21% (with a budget of 10Wh/day) on average. In the target CI mode shown in Figure 8, AutCam’s energy consumption is lower by 37% (with 15% mean CI width) and 35% (with 25% mean CI width) on average.

The improvements of AutCam over UniNN mainly come from two aspects. First, UniNN only uses one single NN counter that performs best globally. However, the optimal choice of NN counter varies across different aggregation windows as shown in §3.3 and Figure 2. Instead, AutCam utilizes the energy/CI front to select the proper NN counter for each individual aggregation window. We observe that for each planning horizon, AutCam deploys 2–5 different NN counters, and the choice of NN counters further varies across different videos and operation constrains. Second, UniNN statically allocates the same energy amount on each aggregation window. However, the video characteristics are disparate across time, and the return of allocating the same amount of energy vary a lot across different aggregation windows as shown in §3.3 and Figure 2. As comparison, AutCam identifies such disparity and judiciously allocates energy among aggregation windows (§4).

7.3.3 Forecasting frame amounts to capture. (§4.2.1) AutCam significantly outperforms CapAll, which makes sampling plan as AutCam but without forecasting frame quantity online (capture every frame). In the energy mode shown in Figure 7, AutCam’s CI width is smaller by 16% (with a budget of 30Wh/day) and 21% (with a budget of 47Wh/day) on average. In the target CI mode shown in Figure 8, AutCam’s energy consumption is lower by 26% (with 15% mean CI width) and 55% (with 25% mean CI width) on average.

Though CapAll shares the techniques of selecting NN counter and energy allocation as AutCam, it spends too much energy on image capturing. Figure 8 breaks down the overall energy consumption into two main parts: image capture and processing. On most approaches except CapAll, the capture energy only contributes to 2% – 20% (8.4% on average) of the total energy consumption. The reason is that GoldenNN and UniNN only capture the number that will be processed, while AutCam uses a fine-grained forward planning approach to determine how many frames are likely needed. The results show that AutCam only has 14.7% of its captured images wasted on average (planning terminates before those images are processed). As comparison, CapAll spends 35.4%, 62.1%, and 72.8% of its energy on image capturing as it captures every frame but only processes less than 20% of them. The above result validates the need of forward planning.

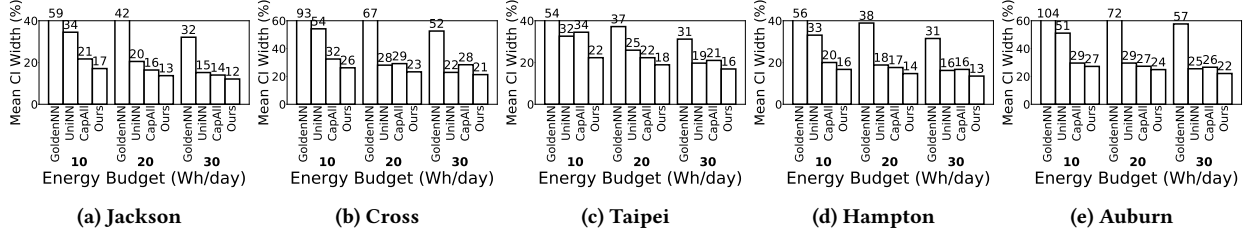


Figure 7: With given energy budgets (X-axis), AutCam provides narrower CIs (Y-axis) than all alternatives.

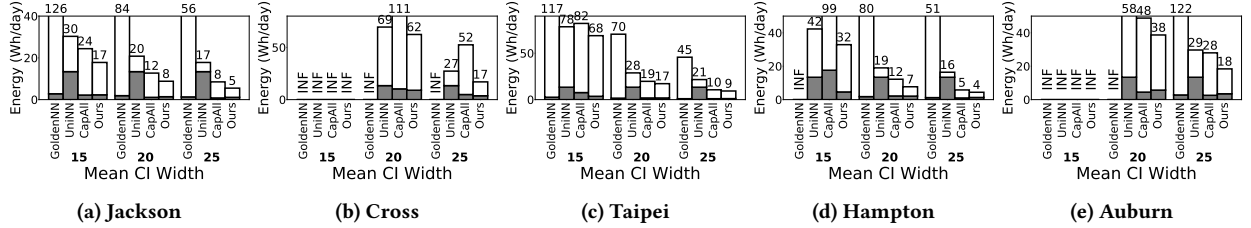


Figure 8: With target CI widths (X-axis), AutCam consumes much lower energy (Y-axis) than all alternatives. The energy is broken down into capture energy (bottom) and processing energy (top). “INF” indicates that the target CI cannot be reached.

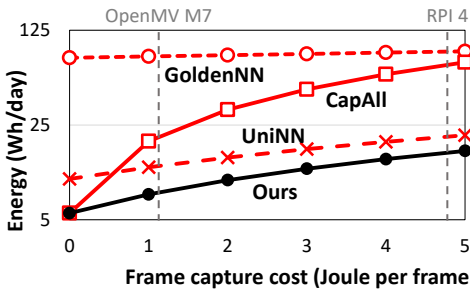


Figure 9: AutCam still consumes less energy than alternatives as the frame capture cost increases. Note: UniNN is an idealistic, impractical design as explained in §7.1. Video: Hampton; CI target: 20%.

The impact of frame capture energy We consider capture energy as the system energy consumption of the whole capture procedure, including boot (resume) and capture. The capture energy varies across hardware as discussed in §6, e.g., ~ 1.2 J on OpenMV M7 or ~ 4.8 J on RPI 4.

As shown in Figure 9, the capture energy has significant impacts on AutCam and other alternatives. When capture energy is zero (a trend towards more energy-efficient hardware to capture image), AutCam and CapAll performs similarly, both much better than UniNN. In this case, AutCam and CapAll carry out an idealistic planning as discussed in §4.1. As the frame capture becomes expensive from zero to 5J, the energy consumption of CapAll quickly increases by 14x, because it spends high energy to exhaustively capture every frame. Though AutCam still outperforms alternatives, the gap between AutCam and GoldenNN is smaller. The reason is that the benefits of using cheap NN counter decreases as it also requires more images to be captured. The performance gap between AutCam and UniNN

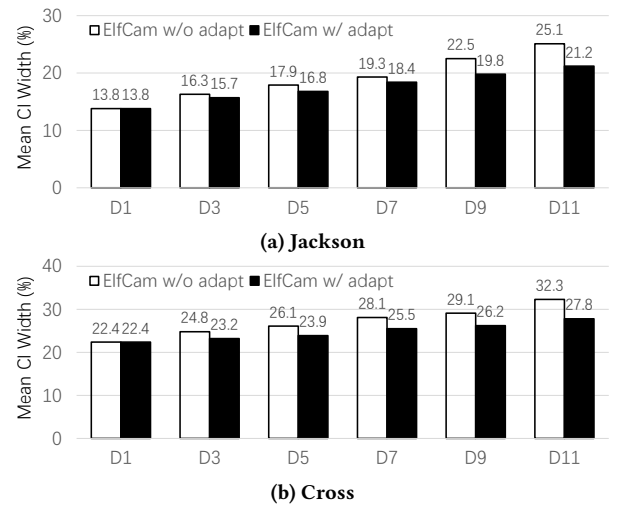


Figure 10: Without renewing its knowledge to changing environment, AutCam’s performance drops across time.

also becomes smaller as the capture energy starts to dominate the overall energy consumption.

7.4 Validation of AutCam adaptiveness

We then study how AutCam performs under changing environments. We run AutCam on two videos, Jackson and Cross, with the energy budget gradually drops from 30Wh/day to 10Wh/day. We report the mean CI width on every two days with and without renewing the knowledge (§4.2.2).

As shown in Figure 10, AutCam’s performance drops as the energy budget becomes tighter on both videos due to the reduced

number of processed frames. However, with AutCam's adaptiveness through knowledge renewing, the mean CI width only increases by 7.4% and 5.4% on Jackson and Cross, respectively. Turning off the adaptiveness, the mean CI width increases become 8.3% and 9.9%. As we observed, the main difference is that, without adapting to the reducing energy budget, AutCam captures excessive frames during but has no enough energy to process them.

8 RELATED WORK

Optimizing video analytics Many systems have been proposed for real-time [41, 59, 67, 84, 96, 97, 101, 103] or retrospective video analytics [56, 58, 60, 83, 98, 99]. However, most of these systems are designed to run on cloud/edge, while a few of them co-run on both camera (often as filters) and cloud/edge [41, 84, 98]. All of them are optimized for low latency or high throughput, with energy ignored. Thus, they have no energy planning across different time windows. Besides, they exhaustively run NNs on every frame, ignoring the opportunity of sampling. As a result, those systems don't fit into the autonomous cameras.

Energy harvesting systems The idea of running modern applications on harvested energy has attracted a lot of research attentions. Hardware and systems have been built towards such scenarios [44, 45, 50–52, 54, 92]. AutCam shares motivation and can borrow certain techniques from them, e.g., forecasting harvested energy. However, most of them assume batteryless platforms, thus focus on how to balance the workloads and harvested energy at realtime. Instead, AutCam is equipped with battery so that it can plan energy over many time windows, an opportunity ignored by most prior work.

Recently, many self-powered cameras are built by research community [73–76, 78] and industry [3, 11, 22]. Those cameras, however, can only capture and stream images to nearby devices, or running lightweight analytics such as background subtraction. Differently, AutCam is designed to analyze videos using state-of-the-art NN object detectors. Running those NNs is much more energy-intensive, thus requires more aggressive and domain-specific techniques, e.g., sampling.

Answering statistical query with approximation and sampling Approximate query processing (AQP) [49] has been proposed to reduce the query delay on large-scale data. Typical AQP approaches include online aggregation (OLA) [35, 46, 53, 81] and offline synopses generation [32, 33, 43]. Besides, many sampling strategies [31, 37, 43, 91, 100] have been proposed to improve the query performance. Those systems answer queries with approximation and bounded error as AutCam does. However, AutCam deploys another dimension of approximation by utilizing inaccurate but cheap NNs, which opens trade-off between sample quality and sample quantity. AutCam also incorporates novel technique (§5) to integrate the errors from different aspects of approximation.

9 CONCLUSIONS

AutCam is an analytics system to answer object counting queries on autonomous cameras. AutCam is the first to combine inaccurate NNs and sampling technique for video query. It consists of a novel mechanism to making heterogeneous sampling decisions within and across multiple time windows; and a novel approach

to integrate errors from different sources. Tested on large-scale videos, AutCam can provide good estimation of object counts with bounded, narrow errors.

REFERENCES

- [1] Privacy fears grow as cities increase surveillance. <https://www.nytimes.com/2013/10/14/technology/privacy-fears-as-surveillance-grows-in-cities.html>, 2013.
- [2] Jetson tx2 module. <https://developer.nvidia.com/embedded/buy/jetson-tx2>, 2018.
- [3] Openmv cam m7. <https://openmv.io/collections/cams/products/openmv-cam-m7>, 2018.
- [4] 5 most inventive uses of computer vision in retail. <https://traxretail.com/2018/06/20/5-inventive-uses-computer-vision-retail/>, 2019.
- [5] Aiy vision kit. <https://aiyprojects.withgoogle.com/vision/>, 2019.
- [6] Arlo pro 2: battery-powered camera. <https://www.arlo.com/en-us/products/arlo-pro-2/default.aspx>, 2019.
- [7] Blink indoor home security camera. <https://blinkforhome.com/collections/blink-security-camera/products/blink-two-camera-system>, 2019.
- [8] Debate: Are video surveillance cameras in public places a good idea. <https://www.debate.org>, 2019.
- [9] Facial recognition machine. <https://www.nytimes.com/interactive/2019/04/16/opinion/facial-recognition-new-york-city.html>, 2019.
- [10] Firefly dl. <https://www.flir.com/products/firefly-dl/>, 2019.
- [11] The first ever battery-free ai technology. <https://www.xnor.ai/solar-powered-ai>, 2019.
- [12] Image processing for precise agriculture. <https://www.rsipvision.com/precise-agriculture/>, 2019.
- [13] imuto portable charger 30000mah power bank. <https://www.amazon.com/Portable-30000mAh-Qualcomm-External-Nintendo/dp/B01LYVF137>, 2019.
- [14] It's time to panic about privacy. <https://www.nytimes.com/interactive/2019/04/10/opinion/internet-data-privacy.html>, 2019.
- [15] Jevois smart machine vision. <https://www.jevoisinc.com/>, 2019.
- [16] Nnpack-accelerated darknet. <https://github.com/digitalbrain79/darknet-nnpack>, 2019.
- [17] OpenCV 3.3. <https://opencv.org/opencv-3-3/>, 2019.
- [18] protests against surveillance cameras. <http://www.notbored.org/camera-protests.html>, 2019.
- [19] Raspberry pi 4. <https://www.raspberrypi.org/products/raspberry-pi-4-model-b/>, 2019.
- [20] Reolink solar panel power supply for wireless outdoor camera. <https://www.amazon.com/Reolink-Solar-Panel-Rechargeable-Waterproof/dp/B0798MV7NS/>, 2019.
- [21] Reolink: Wire-free, with rechargeable battery; solar powered optionally. <https://reolink.com/product/argus-pro/>, 2019.
- [22] Solar powered security camera buyer's guide. <https://reolink.com/solar-powered-security-cameras-buying-guide/>, 2019.
- [23] Vehicle prediction using tensorflow object counting api. https://github.com/ahmetozlu/vehicle_counting_tutorial, 2019.
- [24] Youtube live streaming: Auburn. <https://www.youtube.com/watch?v=hMYIc5ZPJ4>, 2019.
- [25] Youtube live streaming: Cross. <https://www.youtube.com/watch?v=049ltZb9JP8>, 2019.
- [26] Youtube live streaming: Hampton. <https://www.youtube.com/watch?v=y3NOhpkoR-w>, 2019.
- [27] Youtube live streaming: Jackson town. <https://www.youtube.com/watch?v=IEiC9bvVGnk>, 2019.
- [28] Youtube live streaming: Taipei. <https://www.youtube.com/watch?v=1y5dcfnv-Ss>, 2019.
- [29] Martin Abadi, Paul Barham, Jianmin Chen, Zhifeng Chen, Andy Davis, Jeffrey Dean, Matthieu Devin, Sanjay Ghemawat, Geoffrey Irving, Michael Isard, Manjunath Kudlur, Josh Levenberg, Rajat Monga, Sherry Moore, Derek G. Murray, Benoit Steiner, Paul Tucker, Vijay Vasudevan, Pete Warden, Martin Wicke, Yuan Yu, and Xiaoqiang Zheng. Tensorflow: A system for large-scale machine learning. In 12th USENIX Symposium on Operating Systems Design and Implementation (OSDI 16), pages 265–283, Savannah, GA, 2016. USENIX Association.
- [30] Kevin Abas, Kafila Obraczka, and Leland Miller. Solar-powered, wireless smart camera network: An iot solution for outdoor video monitoring. *Computer Communications*, 118:217–233, 2018.
- [31] Swarup Acharya, Phillip B Gibbons, and Viswanath Poosala. Congressional samples for approximate answering of group-by queries. In *ACM SIGMOD Record*, volume 29, pages 487–498. ACM, 2000.
- [32] Swarup Acharya, Phillip B Gibbons, Viswanath Poosala, and Sridhar Ramaswamy. The aqua approximate query answering system. In *ACM SIGMOD Record*, volume 28, pages 574–576. ACM, 1999.

[33] Pankaj K Agarwal, Graham Cormode, Zengfeng Huang, Jeff M Phillips, Zhewei Wei, and Ke Yi. Mergeable summaries. *ACM Transactions on Database Systems (TODS)*, 38(4):26, 2013.

[34] Sameer Agarwal, Henry Milner, Ariel Kleiner, Ameet Talwalkar, Michael Jordan, Samuel Madden, Barzan Mozafari, and Ion Stoica. Knowing when you're wrong: building fast and reliable approximate query processing systems. In *Proceedings of the 2014 ACM SIGMOD international conference on Management of data*, pages 481–492. ACM, 2014.

[35] Sameer Agarwal, Barzan Mozafari, Aurojit Panda, Henry Milner, Samuel Madden, and Ion Stoica. Blinkdb: Queries with bounded errors and bounded response times on very large data. In *Proceedings of the 8th ACM European Conference on Computer Systems, EuroSys '13*, pages 29–42, New York, NY, USA, 2013. ACM.

[36] Nitin Agrawal and Ashish Vulimiri. Low-latency analytics on colossal data streams with summarystore. In *Proceedings of the 26th Symposium on Operating Systems Principles, SOSP '17*, pages 647–664, New York, NY, USA, 2017. ACM.

[37] Brian Babcock, Surajit Chaudhuri, and Gautam Das. Dynamic sample selection for approximate query processing. In *Proceedings of the 2003 ACM SIGMOD international conference on Management of data*, pages 539–550. ACM, 2003.

[38] David Beymer, Philip McLauchlan, Benjamin Coifman, and Jitendra Malik. A real-time computer vision system for measuring traffic parameters. In *Proceedings of IEEE computer society conference on computer vision and pattern recognition*, pages 495–501. IEEE, 1997.

[39] Anil Bhattacharyya. On a measure of divergence between two statistical populations defined by their probability distributions. *Bull. Calcutta Math. Soc.*, 35:99–109, 1943.

[40] Debojith Biswas, Hongbo Su, Chengyi Wang, Jason Blankenship, and Aleksandar Stevanovic. An automatic car counting system using overfeat framework. *Sensors*, 17(7):1535, 2017.

[41] Christopher Canel, Thomas Kim, Giulio Zhou, Conglong Li, Hyeontaek Lim, David G. Andersen, Michael Kaminsky, and Subramanya R. Dulloor. Scaling video analytics on constrained edge nodes. In *Proceedings of the 2nd SysML Conference*, 2019.

[42] Kaushik Chakrabarti, Minos Garofalakis, Rajeev Rastogi, and Kyuseok Shim. Approximate query processing using wavelets. *The VLDB Journal—The International Journal on Very Large Data Bases*, 10(2–3):199–223, 2001.

[43] Surajit Chaudhuri, Gautam Das, and Vivek Narasayya. Optimized stratified sampling for approximate query processing. *ACM Transactions on Database Systems (TODS)*, 32(2):9, 2007.

[44] Alexei Colin, Graham Harvey, Brandon Lucia, and Alanson P Sample. An energy-interference-free hardware-software debugger for intermittent energy-harvesting systems. *ACM SIGPLAN Notices*, 51(4):577–589, 2016.

[45] Alexei Colin, Emily Ruppel, and Brandon Lucia. A reconfigurable energy storage architecture for energy-harvesting devices. In *ACM SIGPLAN Notices*, volume 53, pages 767–781. ACM, 2018.

[46] Tyson Condie, Neil Conway, Peter Alvaro, Joseph M. Hellerstein, Khaled Elmehreky, and Russell Sears. Mapreduce online. In *Proceedings of the 7th USENIX Conference on Networked Systems Design and Implementation, NSDI'10*, pages 21–21, Berkeley, CA, USA, 2010. USENIX Association.

[47] Wilfrid J Dixon and Frank J Massey Jr. Introduction to statistical analysis. 1951.

[48] Frédéric Dufaux and Touradj Ebrahimi. A framework for the validation of privacy protection solutions in video surveillance. In *2010 IEEE International Conference on Multimedia and Expo*, pages 66–71. IEEE, 2010.

[49] Minos N Garofalakis and Phillip B Gibbons. Approximate query processing: Taming the terabytes. In *VLDB*, pages 343–352, 2001.

[50] Graham Gobieski, Brandon Lucia, and Nathan Beckmann. Intelligence beyond the edge: Inference on intermittent embedded systems. In *Proceedings of the Twenty-Fourth International Conference on Architectural Support for Programming Languages and Operating Systems*, pages 199–213. ACM, 2019.

[51] Iñigo Goiri, William Katsak, Kien Le, Thu D Nguyen, and Ricardo Bianchini. Designing and managing data centers powered by renewable energy. *IEEE Micro*, 34(3):8–16, 2014.

[52] Iñigo Goiri, Kien Le, Thu D Nguyen, Jordi Guitart, Jordi Torres, and Ricardo Bianchini. Greenhadoop: leveraging green energy in data-processing frameworks. In *Proceedings of the 7th ACM european conference on Computer Systems*, pages 57–70. ACM, 2012.

[53] Joseph M. Hellerstein, Peter J. Haas, and Helen J. Wang. Online aggregation. In *Proceedings of the 1997 ACM SIGMOD International Conference on Management of Data, SIGMOD '97*, pages 171–182, New York, NY, USA, 1997. ACM.

[54] Josiah Hester, Travis Peters, Tianlong Yun, Ronald Peterson, Joseph Skinner, Bhargav Golla, Kevin Storer, Steven Hearndon, Kevin Freeman, Sarah Lord, et al. Amulet: An energy-efficient, multi-application wearable platform. In *Proceedings of the 14th ACM Conference on Embedded Network Sensor Systems CD-ROM*, pages 216–229. ACM, 2016.

[55] Jarrod C Hodgson, Shane M Baylis, Rowan Mott, Ashley Herrod, and Rohan H Clarke. Precision wildlife monitoring using unmanned aerial vehicles. *Scientific reports*, 6:22574, 2016.

[56] Kevin Hsieh, Ganesh Ananthanarayanan, Peter Bodik, Shivaram Venkataraman, Paramvir Bahl, Matthai Philipose, Phillip B. Gibbons, and Onur Mutlu. Focus: Querying large video datasets with low latency and low cost. In *13th USENIX Symposium on Operating Systems Design and Implementation (OSDI '18)*, Carlsbad, CA, 2018. USENIX Association.

[57] Meng-Ru Hsieh, Yen-Liang Lin, and Winston H Hsu. Drone-based object counting by spatially regularized regional proposal network. In *Proceedings of the IEEE International Conference on Computer Vision*, pages 4145–4153, 2017.

[58] Samvit Jain, Junchen Jiang, Yuanchao Shu, Ganesh Ananthanarayanan, and Joseph Gonzalez. Rexcam: Resource-efficient, cross-camera video analytics at enterprise scale. *CoRR*, abs/1811.01268, 2018.

[59] Junchen Jiang, Ganesh Ananthanarayanan, Peter Bodik, Siddhartha Sen, and Ion Stoica. Chameleon: Scalable adaptation of video analytics. In *Proceedings of the 2018 Conference of the ACM Special Interest Group on Data Communication, SIGCOMM '18*, pages 253–266, New York, NY, USA, 2018. ACM.

[60] Daniel Kang, John Emmons, Firas Abuzaid, Peter Bailis, and Matei Zaharia. Noscope: Optimizing neural network queries over video at scale. *Proc. VLDB Endow.*, 10(11):1586–1597, August 2017.

[61] Sitanshu Sekhar Kar and Archana Ramalingam. Is 30 the magic number? issues in sample size estimation. *National Journal of Community Medicine*, 4(1):175–179, 2013.

[62] P Karpagavalli and AV Ramprasad. Estimating the density of the people and counting the number of people in a crowd environment for human safety. In *2013 International Conference on Communication and Signal Processing*, pages 663–667. IEEE, 2013.

[63] Jay Kreps, Neha Narkhede, Jun Rao, et al. Kafka: A distributed messaging system for log processing. In *Proceedings of the NetDB*, pages 1–7, 2011.

[64] Tsung-Yi Lin, Michael Maire, Serge Belongie, James Hays, Pietro Perona, Deva Ramanan, Piotr Dollár, and C Lawrence Zitnick. Microsoft coco: Common objects in context. In *European conference on computer vision*, pages 740–755. Springer, 2014.

[65] Alan J Lipton, Peter L Venetianer, Niels Haering, Paul C Brewer, Weihong Yin, Zhong Zhang, Li Yu, Yongtong Hu, Gary W Myers, Andrew J Chosak, et al. Video analytics for retail business process monitoring, October 13 2015. US Patent 9,158,975.

[66] Fei Liu, Zhiyuan Zeng, and Rong Jiang. A video-based real-time adaptive vehicle-counting system for urban roads. *PloS one*, 12(11):e0186098, 2017.

[67] Peng Liu, Bozhao Qi, and Suman Banerjee. Edgeeye: An edge service framework for real-time intelligent video analytics. In *Proceedings of the 1st International Workshop on Edge Systems, Analytics and Networking, EdgeSys'18*, pages 1–6, New York, NY, USA, 2018. ACM.

[68] Wei Liu, Dragomir Anguelov, Dumitru Erhan, Christian Szegedy, Scott Reed, Cheng-Yang Fu, and Alexander C Berg. Ssd: Single shot multibox detector. In *European conference on computer vision*, pages 21–37. Springer, 2016.

[69] Xu Liu, Zilei Wang, Jiashi Feng, and Hongsheng Xi. Highway vehicle counting in compressed domain. In *Proceedings of the IEEE Conference on Computer Vision and Pattern Recognition*, pages 3016–3024, 2016.

[70] Xiaolei Ma, Zhuang Dai, Zhengbing He, Jihui Ma, Yong Wang, and Yunpeng Wang. Learning traffic as images: a deep convolutional neural network for large-scale transportation network speed prediction. *Sensors*, 17(4):818, 2017.

[71] Aleksander Maricq, Dmitry Duplyakin, Ivo Jimenez, Carlos Malzahn, Ryan Stutsman, and Robert Ricci. Taming performance variability. In *13th {USENIX} Symposium on Operating Systems Design and Implementation ({OSDI} '18)*, pages 409–425, 2018.

[72] Michael C Mongeon, Robert Paul Loce, and Matthew Adam Shreve. Busyness deflection and notification method and system, February 21 2017. US Patent 9,576,371.

[73] Saman Naderiparizi, Mehrdad Hessar, Vamsi Talla, Shyamnath Gollakota, and Joshua R Smith. Towards battery-free {HD} video streaming. In *15th {USENIX} Symposium on Networked Systems Design and Implementation ({NSDI} '18)*, pages 233–247, 2018.

[74] Saman Naderiparizi, Zerina Kapetanovic, and Joshua R Smith. Battery-free connected machine vision with wiscam. *GetMobile: Mobile Computing and Communications*, 20(1):10–13, 2016.

[75] Saman Naderiparizi, Aaron N Parks, Zerina Kapetanovic, Benjamin Ransford, and Joshua R Smith. Wiscam: A battery-free rfid camera. In *2015 IEEE International Conference on RFID (RFID)*, pages 166–173. IEEE, 2015.

[76] Saman Naderiparizi, Yi Zhao, James Youngquist, Alanson P Sample, and Joshua R Smith. Self-localizing battery-free cameras. In *Proceedings of the 2015 ACM International Joint Conference on Pervasive and Ubiquitous Computing*, pages 445–449. ACM, 2015.

[77] Milind Naphade, David C Anastasiu, Anuj Sharma, Vamsi Jagrlamudi, Hyeran Jeon, Kaikai Liu, Ming-Ching Chang, Siwei Lyu, and Zeyu Gao. The nvidia ai city challenge. In *2017 IEEE SmartWorld, Ubiquitous Intelligence & Computing*.

Advanced & Trusted Computed, Scalable Computing & Communications, Cloud & Big Data Computing, Internet of People and Smart City Innovation (SmartWorld/SCALCOM/UIC/ATC/CBDCom/IOP/SCI), pages 1–6. IEEE, 2017.

[78] Shree K Nayar, Daniel C Sims, and Mikhail Fridberg. Towards self-powered cameras. In 2015 IEEE International Conference on Computational Photography (ICCP), pages 1–10. IEEE, 2015.

[79] Mohammad Sadegh Norouzzadeh, Anh Nguyen, Margaret Kosmala, Alexandra Swanson, Meredith S Palmer, Craig Packer, and Jeff Clune. Automatically identifying, counting, and describing wild animals in camera-trap images with deep learning. *Proceedings of the National Academy of Sciences*, 115(25):E5716–E5725, 2018.

[80] Min-hwan Oh, Peder A Olsen, and Karthikeyan Natesan Ramamurthy. Crowd counting with decomposed uncertainty. *arXiv preprint arXiv:1903.07427*, 2019.

[81] Niketan Pansare, Vinayak R Borkar, Chris Jermaine, and Tyson Condie. Online aggregation for large mapreduce jobs. *Proc. VLDB Endow.*, 4(11):1135–1145, 2011.

[82] Jason Remington Parham, Jonathan Crall, Charles Stewart, Tanya Berger-Wolf, and Daniel Rubenstein. Animal population censusing at scale with citizen science and photographic identification. In *2017 AAAI Spring Symposium Series*, 2017.

[83] Alex Poms, Will Crichton, Pat Hanrahan, and Kayvon Fatahalian. Scanner: Efficient video analysis at scale. *ACM Trans. Graph.*, 37(4):138:1–138:13, July 2018.

[84] X. Ran, H. Chen, X. Zhu, Z. Liu, and J. Chen. Deepdecision: A mobile deep learning framework for edge video analytics. In *IEEE INFOCOM 2018 - IEEE Conference on Computer Communications*, pages 1421–1429, April 2018.

[85] Joseph Redmon and Ali Farhadi. Yolo9000: better, faster, stronger. In *Proceedings of the IEEE conference on computer vision and pattern recognition*, pages 7263–7271, 2017.

[86] Joseph Redmon and Ali Farhadi. Yolov3: An incremental improvement. *arXiv preprint arXiv:1804.02767*, 2018.

[87] Shaogang Ren, Kaiming He, Ross Girshick, and Jian Sun. Faster r-cnn: Towards real-time object detection with region proposal networks. In *Advances in neural information processing systems*, pages 91–99, 2015.

[88] Reuven Y Rubinstein and Dirk P Kroese. *Simulation and the Monte Carlo method*, volume 10. John Wiley & Sons, 2016.

[89] Mark Sandler, Andrew Howard, Menglong Zhu, Andrey Zhmoginov, and Liang-Chieh Chen. Mobilenetv2: Inverted residuals and linear bottlenecks. In *Proceedings of the IEEE Conference on Computer Vision and Pattern Recognition*, pages 4510–4520, 2018.

[90] Honghui Shi. Geometry-aware traffic flow analysis by detection and tracking. In *Proceedings of the IEEE Conference on Computer Vision and Pattern Recognition Workshops*, pages 116–120, 2018.

[91] Lefteris Sidiropoulos, PA Boncz, ML Kersten, et al. Sciborg: Scientific data management with bounds on runtime and quality, 2011.

[92] Rahul Singh, David Irwin, Prashant Shenoy, and Kadangode K Ramakrishnan. Yank: Enabling green data centers to pull the plug. In *Presented as part of the 10th {USENIX} Symposium on Networked Systems Design and Implementation ({NSDI} 13)*, pages 143–155, 2013.

[93] Madjid Tavana and Srikanta Patnaik. *Recent Developments in Data Science and Business Analytics*. Springer, 2018.

[94] Jan C van Gemert, Camiel R Verschoor, Pascal Mettes, Kitso Epema, Lian Pin Koh, and Serge Wich. Nature conservation drones for automatic localization and counting of animals. In *European Conference on Computer Vision*, pages 255–270. Springer, 2014.

[95] Deepak Vasish, Zerina Kapetanovic, Jongho Won, Xinxin Jin, Ranveer Chandra, Sudipta Sinha, Ashish Kapoor, Madhusudhan Sudarshan, and Sean Stratman. Farmbeats: An iot platform for data-driven agriculture. In *14th {USENIX} Symposium on Networked Systems Design and Implementation ({NSDI} 17)*, pages 515–529, 2017.

[96] Junjue Wang, Brandon Amos, Anupam Das, Padmanabhan Pillai, Norman Sadeh, and Mahadev Satyanarayanan. A scalable and privacy-aware iot service for live video analytics. In *Proceedings of the 8th ACM on Multimedia Systems Conference, MMSys'17*, pages 38–49, New York, NY, USA, 2017. ACM.

[97] Junjue Wang, Ziqiang Feng, Zhuo Chen, Shilpa George, Mihir Bala, Padmanabhan Pillai, Shao-Wen Yang, and Mahadev Satyanarayanan. Bandwidth-efficient live video analytics for drones via edge computing. In *2018 IEEE/ACM Symposium on Edge Computing, SEC 2018, Seattle, WA, USA, October 25–27, 2018*, pages 159–173, 2018.

[98] Mengwei Xu, Tianfu Xu, Yunxin Liu, Xuanze Liu, Gang Huang, and Felix Xiaozhu Lin. Supporting video queries on zero-streaming cameras. *arXiv preprint arXiv:1904.12342*, 2019.

[99] Tianfu Xu, Luis Materon Botelho, and Felix Xiaozhu Lin. Vstore: A data store for analytics on large videos. In *Proceedings of the Fourteenth EuroSys Conference 2019, EuroSys'19*, pages 16:1–16:17, New York, NY, USA, 2019. ACM.

[100] Ying Yan, Liang Jeff Chen, and Zheng Zhang. Error-bounded sampling for analytics on big sparse data. *Proceedings of the VLDB Endowment*, 7(13):1508–1519, 2014.

[101] S. Yi, Z. Hao, Q. Zhang, Q. Zhang, W. Shi, and Q. Li. Lavea: Latency-aware video analytics on edge computing platform. In *2017 IEEE 37th International Conference on Distributed Computing Systems (ICDCS)*, pages 2573–2574, June 2017.

[102] B Yogameena and C Nagananthini. Computer vision based crowd disaster avoidance system: A survey. *International journal of disaster risk reduction*, 22:95–129, 2017.

[103] Haoyu Zhang, Ganesh Ananthanarayanan, Peter Bodik, Matthai Philipose, Paramvir Bahl, and Michael J. Freedman. Live video analytics at scale with approximation and delay-tolerance. In *14th USENIX Symposium on Networked Systems Design and Implementation (NSDI 17)*, pages 377–392, Boston, MA, 2017. USENIX Association.

[104] Yingying Zhang, Desen Zhou, Siqin Chen, Shenghua Gao, and Yi Ma. Single-image crowd counting via multi-column convolutional neural network. In *Proceedings of the IEEE conference on computer vision and pattern recognition*, pages 589–597, 2016.

[105] Hongwei Zhu, Farzin Aghdasi, Greg M Millar, and Stephen J Mitchell. Online learning method for people detection and counting for retail stores, May 2 2017. US Patent 9,639,747.